Hydrolytic dehydrogenation of ammonia borane over ZIF-67 derived Co nanoparticle catalysts

Zacho, Simone Louise; Mielby, Jerrik Jørgen; Kegnæs, Søren

Published in:
Catalysis Science & Technology

Link to article, DOI:
10.1039/C8CY01500G

Publication date:
2018

Document Version
Peer reviewed version

Catalysis Science & Technology

Accepted Manuscript

This article can be cited before page numbers have been issued, to do this please use: S. L. Zacho, J. Mielby and S. Kegnæs, *Catal. Sci. Technol.*, 2018, DOI: 10.1039/C8CY01500G.

ROYAL SOCIETY OF CHEMISTRY

rsc.li/catalysis

View Article Online
DOI: 10.1039/C8CY01500G

Journal Name

ARTICLE

Hydrolytic dehydrogenation of ammonia borane over ZIF-67 derived Co nanoparticle catalysts

Received 00th January 20xx,
Accepted 00th January 20xx

DOI: 10.1039/x0xx00000x

www.rsc.org/

Simone Louise Zacho,[a] Jerrik Mielby[a] and Søren Kegnæs[a]*

In this work, we exploited zeolitic imidazolate framework ZIF-67 as sacrificial precursors to prepare Co nanoparticles supported on nanoporous nitrogen-doped carbon. The catalysts were tested for hydrolytic dehydrogenation of ammonia borane and the size of the Co nanoparticles and the structural features of the carbon support were shown to have a large effect on the catalytic activity. Furthermore, we investigated the effect of adding Zn to the catalyst precursor (ZIF-67/8). The highest catalytic activity was obtained from ZIF-67/8 with a molar ratio of Co/Zn=1, which was carbonized at 900°C to remove Zn by evaporation. At room temperature, this catalyst resulted in a turnover frequency of 7.6 mol H_2/mol Co min^{-1} and an apparent activation energy of E_a=44.9 kJ/mol. The turnover frequency was further increased to 12.7 min^{-1} in 0.1 M NaOH.

Introduction

Hydrogen produced from renewable resources holds great promise as a solution to future energy and environmental challenges.[1] In particular, hydrogen may power fuel cells, which can generate electricity without emission of greenhouse gasses. Unfortunately, the physical properties of hydrogen gas make transportation, handling and refuelling difficult. Much effort has therefore been devoted to the development of chemical hydrogen storage materials.[2,3,4,5] In these types of materials, chemical processes control hydrogen storage and release. This makes them different from metal hydrides[6] or carbon materials,[7] where temperature and pressure control storage and release. One compound, ammonia borane (H_3NBH_3), has attracted particular attention because of its high volumetric and gravimetric density. Ammonia borane is solid at room temperature, stable in air and water and contains around 196 g/kg or 100-140 g/l of H_2.[8] In combination with an efficient catalyst, the hydrolytic dehydrogenation of ammonia borane is given by

1) $H_3NBH_3\ (aq) + 2H_2O\ (l) \rightarrow NH_4(BO_2)(aq) + 3H_2(g)$

In a protic solvent like H_2O, up to three equivalents of H_2 can be released from ammonia borane and when a proper catalyst is used, hydrogen can be released under ambient conditions. In the past years, a number of efficient noble metal catalysts have been developed for the hydrolytic dehydrogenation of H_3NBH_3, including both homogeneous[9] and heterogeneous catalysts based on Pt,[10] Rh,[11] Ru,[12] Ag[13] and Pd[14]. Considering the limited availability and high cost of noble metals, the development of equally active and more cost-effective non-noble metal catalysts is of great interest.[15] Among the non-noble metals, Co supported on carbon has recently been suggested as a promising catalyst because of its high activity[16] and magnetic properties. These properties make is easy to collect the supported nanoparticles from the liquid phase.[17,18,19] For instance, Wang *et al*.[20] recently embedded Co nanoparticles in porous nitrogen-doped carbon, which was synthesized by carbonization of a Co(salen) precursor under Ar atmosphere. The Co nanoparticles resulted in a turnover frequency (TOF) of 5.6 mol H_2/mol Co min^{-1} in the hydrolytic dehydrogenation of ammonia borane. The catalyst showed good stability over 10 runs collecting the catalyst using a permanent magnet after each run. The porosity of these type of carbon materials is a key factor for the catalytic activity.

Here, we report a method to prepare Co nanoparticles supported on a porous nitrogen-doped carbon matrix synthesized by carbonization. The method exploits metal organic frameworks (MOFs) as sacrificial precursors for both the cobalt nanoparticles and the nitrogen-doped carbon matrix support. Because of their remarkable chemical and structural properties, such as their high surface area and well-defined porosity, MOFs have recently attracted much interest for applications in gas adsorption, separation and heterogeneous catalysis.[21,22] Furthermore, MOFs have recently been used for preparation of high-surface area nanoporous carbons for electrochemical reactions.[23]

In this work, we carbonized different zeolitic imidazolate frameworks comprised of Co and 2-methylimidazole (ZIF-67) and investigated the catalytic effect of the particle size and the carbonization temperature. Furthermore, we investigated the

[a] S. L. Zacho, Dr. J. Mielby, Prof. S. Kegnæs
DTU Chemistry, Technical University of Denmark
Kemitorvet Building 207
DK-2800 Kgs. Lyngby, Denmark

Electronic Supplementary Information (ESI) available: [details of any supplementary information available should be includ
ed here]. See DOI: 10.1039/x0xx00000x

View Article Online
DOI: 10.1039/C8CY01500G

effect of adding Zn (bimetallic hybrid of ZIF-67/8) in order to control the Co loading in the catalyst precursor. We carbonized the ZIFs at high temperatures to remove the Zn by evaporation according to Yin *et al.*[24] The best catalyst resulted in a turnover frequency of 7.6 mol H_2/mol Co min^{-1} at room temperature without base. The activity was further tested in 0.1 M NaOH and KOH, which increased the TOF to 12.7 min^{-1} in 0.1 M NaOH and 11.0 min^{-1} in 0.1 M KOH in agreement with previous reports.[25,26]

Experimental

Materials. All reagents were purchased from commercial source (Sigma-Aldrich) and used without further purifications, including $Co(NO_3)_2{\cdot}6H_2O$ (>99.9%), $Zn(NO_3)_2{\cdot}6H_2O$ (>99.9%), 2-methylimidazole (99%), methanol (HPLC Plus, ≥99.9%) and ammonia borane (H_3NBH_3, 97%).

Synthesis of ZIF-67. ZIF-67 was synthesized in methanol according to the literature.[27] In brief, $Co(NO_3)_2{\cdot}6H_2O$ (1.436 g) and 2-methylimidazole (3.244 g) were each dissolved in 100 mL of methanol. The Co salt solution was then poured into the ligand solution and vigorously stirred in a round-bottomed flask for 12 min at the desired temperature (25°C or 60°C). The solution was left without stirring for 24h at 25°C. The purple product was collected by centrifugation, thoroughly washed with methanol three times and then dried at 80°C for 24h. The yield of ZIF-67 was 75% based on the amount of Co. The synthesis temperatures (25°C or 60°C) yielded ZIF-67 with crystal sizes of 300 nm and 500 nm respectively (ZIF-67-300 and ZIF-67-500).

Synthesis of ZIF-67/8. The bimetallic hybrid of ZIF-67 and ZIF-8 (ZIF-67/8) was synthesized with a ratio of Co/Zn=1. The material was prepared according to the synthesis of pure ZIF-67, except that the salt solution consisted of both $Co(NO_3)_2{\cdot}6H_2O$ (0.718 g) and $Zn(NO_3)_2{\cdot}6H_2O$ (0.734 g). After the synthesis, the purple product was collected, washed and dried as described above. The yield of ZIF-67/8 was 79% based on the amount of Co and Zn. The synthesis yielded ZIF-67/8 with an average crystal size of 50 nm (ZIF-67/8-50).

Synthesis of carbonised catalysts. ZIF-67 and ZIF-67/8 were carbonized in a tube furnace at a temperature of 750°C or 900°C for 2 hours under Ar using a heating ramp of 5°C/min. The final catalysts were labelled according to the rough size of the parent catalyst precursor in nm. Figure 1 illustrates the two steps of the synthesis, including crystallization and carbonization, respectively. **Table 1** shows an outline of all the prepared materials.

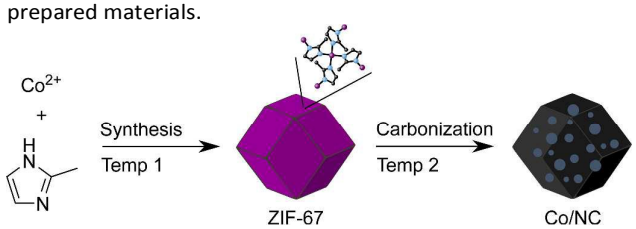

Figure 1. Illustration of the catalyst synthesis.

Table 1. Outline of the prepared materials.

Entry	Step 1	Precursor[a]	Step 2	Catalyst[a]
1	60°C	ZIF-67-500	750°C	Co/NC-500
2	25°C	ZIF-67-300	750°C	Co/NC-300
3	25°C	ZIF-67/8-50	750°C	CoZn/NC-50
4	25°C	ZIF-67/8-50	900°C	Co/NC-50

[a] The names of the prepared materials are distinguished by the crystal sizes of the catalyst precursors (given in nm).

Characterisation. The prepared materials were characterised by X-ray diffraction (XRD), N_2 physisorption, scanning electron microscopy (SEM) and transmission electron microscopy (TEM). Please see supporting information for all experimental details.

Catalytic tests. The catalytic activity was tested in an automated gas burette system equipped with a pressure transducer to follow the displacement of a light silicone oil upon the release of H_2 gas.[28] Before each experiment, 10-20 mg of the catalyst was added to a round bottom flask together with a magnet. The flask was then sealed with a septum and connected to the gas burette system before a solution of 50 mg H_3NBH_3 in 10 ml H_2O was quickly injected into the flask using a syringe. The catalysts were applied without activation by addition of $NaBH_4$, which is commonly used in literature.[20,29,30] The reaction was either stirred at room temperature or heated using an oil bath, while the data were collected and analysed using an online computer. The system was calibrated using a mass flow controller and the release of H_2 calculated from the linear calibration line.

Results and discussion

Figure 2a shows XRD analysis of ZIF-67-300, ZIF-67-500 and ZIF-67/8-50, respectively. The three diffraction patterns show that all catalyst precursors have the characteristic ZIF-67 sodalite structure, with clear and well-resolved peaks at 2θ equal 7° (011), 13° (112) and 18° (222).[24,31] Figure 2b shows the corresponding materials after carbonization Co/NC-300, Co/NC-500 and CoZn/NC-50 at 750°C as well as Co/NC-50 at 900°C. As expected, the carbonization results in a complete decomposition of the crystalline ZIF structure. Here, the XRD shows a broad diffraction band around 20° as well as a smaller band at 26°. We attribute these bands to the diffraction of amorphous carbon with some graphitic-like structure.[32]

View Article Online
DOI: 10.1039/C8CY01500G

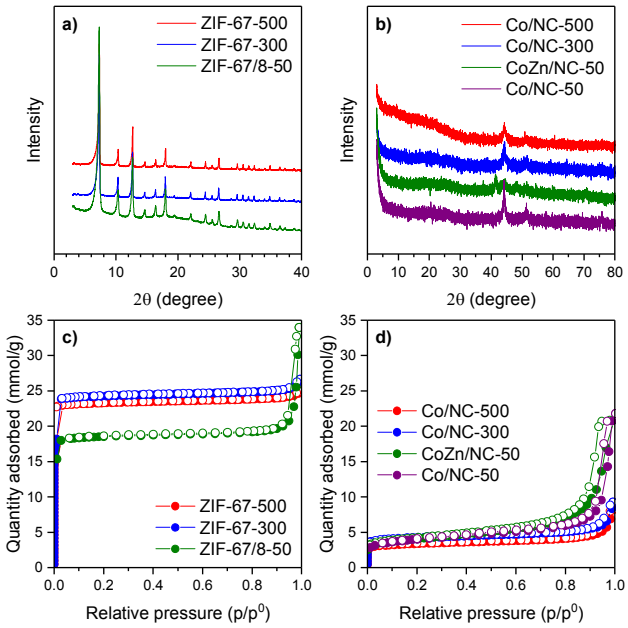

Figure 2. XRD and N_2 physisorption analysis of the prepared materials before (left, a & c) and after carbonization (right, b & d).

Furthermore, the XRD shows three diffraction peaks at 2θ equal 44° Co(111), 52° Co(200) and 76° Co(220), which confirms the formation of face-centred cubic Co nanoparticles.[24] In general, the peaks are too weak to determine the average particle size by line-broadening analysis. Enlarged versions of the XRD patterns of Co/NC-300 and Co/NC-500 are shown in the supporting information.

Figure 2c and 2d show the N_2 physisorption analysis of the catalyst precursors before and after carbonization, respectively. While ZIF-67-500nm and ZIF-67-300nm have type I isotherms, which are typical for MOFs and other microporous materials,[33] ZIF-67/8-50 is absorbing less N_2 at low relative pressures and more N_2 at high relative pressures. We assign the lower micropore volume in ZIF-67/8-50 to the partial substitution of Co by Zn in the framework and the higher mesopore volume to interparticle porosity. After the carbonization, the physisorption analysis results in isotherms with character of both type I and IV. The results from the physisorption analysis are summarised in Table 2 and the corresponding pore size distributions are shown in the supporting information.

Table 2. Summary of results from N_2 physisorption analysis.

Entry	Material	S_{BET} [a] (m^2/g)	S_{ext} [b] (m^2/g)	V_{micro} [b] (cm^3/g)	V_{tot} [d] (cm^3/g)
1	ZIF-67-500	1951	67	0.779	0.842
2	ZIF-67-300	1848	72	0.811	0.884
3	ZIF-67/8-50	1379	90	0.603	0.719
4	Co/NC-500	290	74	0.085	0.210
5	Co/NC-300	356	96	0.103	0.233
6	CoZn/NC-50	335	179	0.065	0.423
7	Co/NC-50	312	184	0.058	0.482

[a] Specific surface area determined by the BET method, [b] external surface area and micropore volume determined by the t-plot method and [d] total pore volume determined by a single point read at p/p^0=0.95.

Figure 3 shows representative SEM images of the prepared materials before (left) and after carbonization under Ar at 750°C for 2h (right). All the catalyst precursors are typical rhombic dodecahedral in shape. Depending on the crystallization temperature, the average crystal size of the ZIF-67 is around 500 nm (for crystallization at 60°C) or around 300 nm (for crystallization at 25°C). By adding $Zn(NO_3)_2$ to the synthesis the average size of the crystals decreases to around 50 nm. After carbonization, Co/NC-500 and Co/NC-300 preserve the shape of their catalyst precursors, although the structures shrink and the sides of the dodecahedrons become more concave. The CoZn-NC-50 catalyst does not retain the shape of its precursor, but appears as larger agglomerates. The corresponding SEM image of Co/NC-50 is similar to CoZn/NC-50 and is shown in the supporting information.

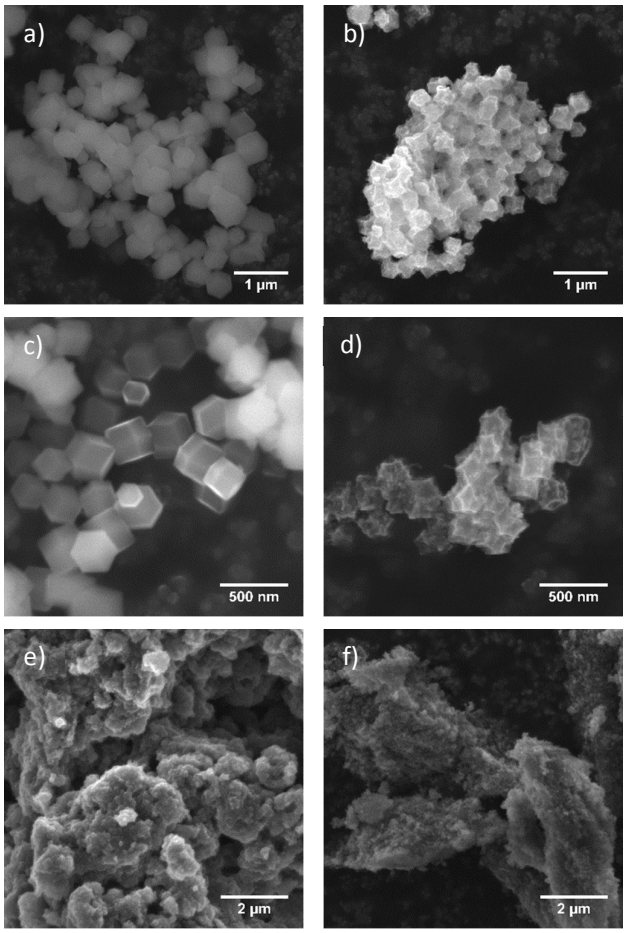

Figure 3. SEM images of a) ZIF-67-500, b) Co/NC-500, c) ZIF-67-300, d) Co/NC-300, e) ZIF-67/8-50 and f) CoZn/NC-50.

View Article Online
DOI: 10.1039/C8CY01500G

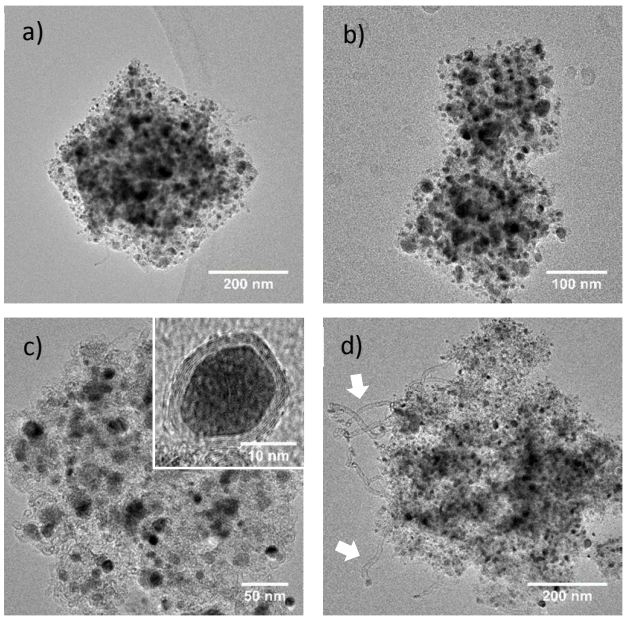

Figure 4. TEM images of a) Co/NC-500, b) Co/NC-300, c) CoZn/NC-50, d) Co/NC-50.

Figure 4 shows representative TEM images of Co/NC-500, Co/NC-300, CoZn/NC-50 and Co/NC-50, respectively. Considering the high metal to carbon ratio, all precursors result in relatively well-dispersed Co nanoparticles, typically in the range of 5-25 nm. While Co/NC-500 and Co/NC-300 have a Co loading of 18 wt%, Co/NC-50 only has a Co loading of 8 wt%. As expected, the nanoparticles in Co/NC-50 are therefore smaller, typically in the range of 5-15 nm. By changing the Co/Zn ratio it is therefore possible to control both the particles size and the Co loading. As reference materials ZIF-67-500 and ZIF-67-300 were also carbonized at 900˚C, which results in large agglomerations of Co nanoparticles with an average size of 100 nm, see supporting information. We speculate that optimisation of the carbonization procedure may result in even smaller nanoparticles. The TEM images also reveal how the carbonization of the catalyst precursors results in the formation of graphitic carbon in Figure 4c and a network of carbon nanotubes that protrudes from the catalyst in Figure 4d. The TEM images of the catalyst precursors ZIF-67-500, ZIF-67-300 and ZIF-67/8-50 are shown in the supporting information.

Figure 5 shows the volume of released H_2 from the catalytic dehydrogenation of ammonia borane over the first 45 min using 20 mg of catalyst and 50 mg of H_3NBH_3 in 10 ml H_2O at 25°C.

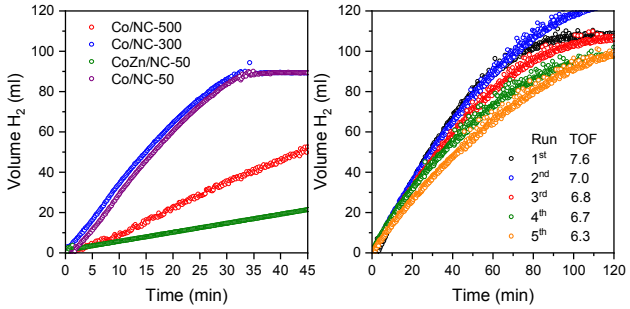

Figure 5. a) Volume of released H_2 from the catalytic dehydrogenation of ammonia borane using 20 mg catalyst at 25°C. b) Recycle tests of Co/NC-50 using 10 mg catalyst. TOF is given in mol H_2/mol Co min^{-1}.

Table 3 shows the corresponding TOF values as calculated from the initial reaction rate and the metal loading (mol H_2/mol Co min^{-1}). While Co/NC-500 only results in a TOF of 1.1 min^{-1}, Co/NC-300 results in a TOF of 2.7 min^{-1}, which may be explained by the higher surface area and porosity of Co/NC-300. These results demonstrate that even small changes in the synthesis of the catalyst precursors can have a significant effect on both the structural and catalytic properties. A similar effect was previously reported by Zou et al. for the oxygen reduction reaction.[34] For both catalysts, the amount of H_2 released per ammonia borane was around 2.4-2.5, which is less than the stoichiometric value of 3 (see equation 1), but in the same range as other non-noble metal catalysts.[15] The reference materials ZIF-67-500 (900˚C) and ZIF-67-300 (900˚C) exhibited low activities in the dehydrogenation of ammonia borane, as expected due to the large agglomerations of Co nanoparticles, see supporting information.

Table 3. Results from the catalytic dehydrogenation of ammonia borane.

Entry	Catalyst	Co wt%[a]	AB/Co[b]	H_2/AB[b]	TOF[c] (min^{-1})
1	Co/NC-500	18	26	2.4	1.1
2	Co/NC-300	18	26	2.5	2.7
3	CoZn/NC-50	4	60	2.7	1.8
4	Co/NC-50	8	126	2.9	7.6

[a] Determined by atomic absorption spectroscopy (AAS). [b] AB=ammonia borane (mol/mol). [c] TOF=turnover frequency (mol H_2/mol Co min^{-1}).

Table 3 shows that the bimetallic CoZn catalyst results in a TOF of 1.8 min^{-1} with a H_2 to ammonia borane ratio of 2.7. It is notable that this catalyst was the least active with respect to the mass of the catalyst as shown in Figure 5. Thus, we speculate that the Zn may form an inactive CoZn alloy in this sample.[35] By increasing the carbonization temperature from 750°C to 900°C, which effectively removes the Zn by evaporation, the TOF increases to 7.6 min^{-1} for Co/NC-50. Furthermore, the released H_2 to ammonia borane ratio increased to around 2.9 of the theoretical 3 equivalents, which corresponds to a yield of 97%.[36,37]

View Article Online
DOI: 10.1039/C8CY01500G

High turnover frequencies have previously been reported for a number of carbon supported Co catalysts, in particular for Co supported on graphene (Co/graphene, TOF=13.9 min^{-1})[29] and Co supported on graphene oxide modified by polyethylenimine (Co/PEI-GO, TOF=39.9 min^{-1}).[30] Common for both systems is that $NaBH_4$ is used to activate the catalysts. Unfortunately, these catalysts were also reported to suffer from severe deactivation retaining only 60-65% of the initial catalytic activity after 5 runs. For comparison, Figure 5 shows how the catalytic activity of Co/NC-50 also decreases over multiple runs. After 5 runs, however, the TOF is still 6.3 min^{-1}, which corresponds to 83% of the initial catalytic activity. Based on TEM analysis we propose that the deactivation may be caused by a combination of particle aggregation and surface oxidation, see supporting information. Wang *et al.* previously reported that their catalyst prepared from Co(Salen) with an initial TOF of 5.6 min^{-1} could be recycled up to 10 times.[20]

Figure 6a shows the effect of increasing the reaction temperature from 25-50°C using the Co/NC-50 catalyst. As expected, the increased temperature has a large effect on the initial reaction rate and at temperatures above 45°C all H_2 is released in less than 25 min. Figure 6b shows the corresponding Arrhenius plot. The apparent activation energy as determined from the slope of the linear fit was calculated to E_a= 44.9 kJ/mol. Yang et al.[8] have previously reported activation energies from 38-67 kJ/mol, which positions the Co/NC-50 catalysts in the better range with respect to the activation energy.

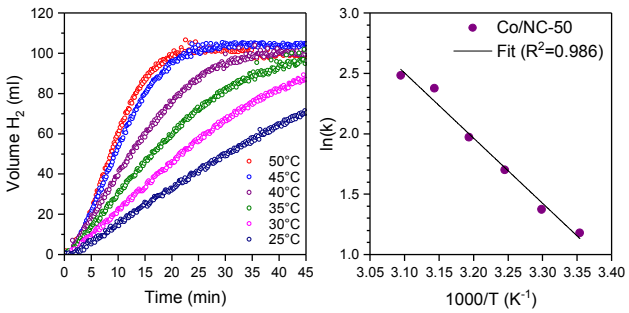

Figure 6. a) Effect of increasing the temperature from 25-50°C and b) the corresponding Arrhenius plot.

In agreement with previous reports,[25] addition of base increased the reaction rate. In 0.1 M KOH the TOF increased to 11.0 min^{-1} and in 0.1 M NaOH the TOF increased to 12.7 min^{-1}, see supporting information.

Conclusions

In conclusion, we exploited the zeolitic imidazolate framework ZIF-67 as sacrificial precursor for the preparation of Co nanoparticles supported on a porous nitrogen-doped carbon matrix. By changing the synthesis temperature, it was possible to control the size of the catalyst precursor crystals and the resulting catalyst particles, which retained the characteristic rhombic dodecahedral shape after carbonization. By addition of Zn to the ZIF synthesis, the size of the precursor crystals decreased to around 50 nm, although the subsequent carbonization resulted in large and undefined agglomerates. The catalysts were tested for the hydrolytic dehydrogenation of ammonia borane and the catalytic activities were related to the size of the Co nanoparticles and the structural features of the carbon support. The highest catalytic activity was obtained from ZIF-67/8 with a molar ratio of Co/Zn=1, which was carbonized at 900°C to remove Zn by evaporation. At room temperature, this catalyst resulted in a turnover frequency of 7.6 mol H_2/mol Co min^{-1} and an apparent activation energy of Ea= 44.9 kJ/mol. Furthermore, it was possible to optimize the reaction in 0.1 M KOH and NaOH, providing a final TOF of 11.0 min^{-1} and 12.7 min^{-1}, respectively. We hope that these results will inspire new perspectives on the exploitation of MOFs as sacrificial precursors and structural templates in heterogeneous catalysis and eventually contribute to the development of more efficient energy technologies.

Conflicts of interest

The author declare no conflicts of interest.

Acknowledgements

The authors are grateful for funding from the Independent Research Fund Denmark (Grant no. 5054-00119 and 6111-00237) and from Villum fonden (Grant No. 13158).

View Article Online
DOI: 10.1039/C8CY01500G

References

1 L. J. Murray, M. Dincă and J. R. Long, *Chem. Soc. Rev.*, 2009, **38**, 1294.
2 L. Klebanoff, 2012 Hydrogen storage technology: materials and applications. Section II, 8. Development of ff-Board Reversible Hydrogen Storage Materials. CRC Press. Boca Raton: Taylor & Francis.
3 A. Klerke, S. K. Klitgaard and R. Fehrmann, *Catal. Lett.*, 2009, **130**, 541-546.
4 J. Mielby, A. J. Kunov-Kruse and S. Kegnæs, *J. Catal.*, 2017, **345**, 149-156.
5 A. Gallas-Hulin, J. Mielby and S. Kegnæs, *ChemistrySelect*, 2016, **1**, 3942-3945.
6 B. Sakintuna, F. Lamari-Darkrim and M. Hirscher, *Int. J. Hydrogen Energy*, 2007, **32**, 1121-1140.
7 Y. Xia, Z. Yang and Y. Zhu *J. Mater. Chem. A*, 2013, **1**, 9365-9381
8 Y. Yang, F. Zhang, H. Wang, Q. Yao, X. Chen and Z. Lu, *J. Nanomater*, 2014, **2014**, 294350.
9 M. Denney, V. Pons, T. Hebden, D. Heinekey and K. Goldberg, *JACS*, 2006, **128**(37), 12048–12049.
10 W. Chen, J. Ji, X. Duan, G. Qian, P. Li, X. Zhou, D. Chen and W. Yuan, *Chem. Commun.* 2014, **50**, 2142−2144.
11 S. Akbayrak, Y. Tonbul and S. Özkar, *Appl. Catal.*, B, 2016, **198**, 162−170.
12 C. Du, Q. Ao, N. Cao, L. Yang, W. Luo and G. Cheng, *Int. J. Hydrogen Energy,* 2015, **40**, 6180−6187.
13 J. Chen, Z.-H. Lu, Y. Wang, X. Chen and L. Zhang, *Int. J. Hydrogen Energy*, 2015, **40**, 4777−4785.
14 S. Akbayrak, M. Kaya, M. Volkan and S. Özkar*, Appl. Catal.,B*, 2014, **147**, 387−393.
15 W. Zhan, Q. Zhu and Q. Xu, *ACS Catal,* 2016, **6(10)**, 6892-6905.
16 J. Hu, Z. Chen, M. Li, X. Zhou and H. Lu, *ACS Appl. Mater. Interfaces*, 2014, **6**, 13191−13200.
17 X. Li, C. Zeng, J. Jiang and L. Ai, *J. Mater. Chem. A*, 2016, **4(19)**, 7476-7482.
18 S. Kramer, J. Mielby, K. Buss, T. Kasama and S. Kegnæs, ChemCatChem, 2017, **9**, 2930-2934.
19 S. Kramer, F. Hejjo, K. H. Rasmussen and S. Kegnæs, *ACS Catal*. 2018, **8**, 754-759.
20 H. Wang, Y. Zhao, F. Cheng, Z. Tao and J. Chen, *Catal. Sci. Technol*, 2016, **6**, 3443- 3448.
21 K. Shen, X. Chen, J. Chen and Y. Li, *ACS Catal.*, 2016, **6(9)**, 5887-5903.
22 B. Chen, Z. Yang, Y. Zhu and Y. Xia, *J. Mater. Chem. A,* 2014, **2(40)**, 16811-16831.
23 B. Liu, H. Shioyama, T. Akita and Q. Xu, *JACS,* 2008, **130(16)**, 5390-5391.
24 P. Yin, T. Yao, Y. Wu, L. Zheng, Y. Lin, W. Liu and Y. Li, *Angew. Chem. Int. Ed*, 2016, **55(36)**, 10800-10805.
25 C. Wang, J. Tuninetti, Z. Wang, C. Zhang, R. Ciganda, L. Salmon and D. Astruc, *JACS*, 2017, **139**(33), 11610–11615.
26 Q. Yao, K. Yang, X. Hong, X. Chen and Z. Lu, *Catal. Sci. Technol.*, 2018, **8**, 870-877.
27 W. Xia, J. Zhu, W. Guo, L. An, D. Xia and R. Zou, *J. Mater. Chem. A* ,2014, **2**, 11606-11613.
28 F. Zheng, S. Rassat, D. Helderandt, D. Cald-well, C. Aardahl, T. Autrey and K. Rappé, *Rev Sci Instrum,* 2008, **79(8)**, 084103.
29 L. Yang, N. Cao, C. Du, H. Dai, K. Hu, W. Luo and G. Cheng, *Mater. Lett.,* 2014, **115**, 113-116.
30 J. Hu, Z. Chen, M. Li, X. Zhou and H. Lu, *ACS Appl. Mater. Interfaces*, 2014, **6**, 13191-13200.
31 X. Feng, and M. Carreon, *J. Cryst. Growth,* 2015, **418**, 158-162.
32 J. Meng, C. Niu, L. Xu, J. Li, X. Liu, X. Wang and L. Mai, *JACS*, 2017, **139**(24), 8212–8221.
33 K. Sing, and R. Williams, 2004, *Adsorpt. Sci. Technol.*, **22(10)**, 773-782.
34 W. Xia, J. Zhu, W. Guo, L. An, D. Xia and R. Zou, *J. Mater. Chem. A*, 2014, 2, 11606.
35 W. Feng, Y. Wang, J. Chen, B. Li, L. Guo, J. Ouyang, D. Jia, Y. Zhou, *J. Mater. Chem. C*, 2018, **6**, 10-18.
36 Ö. Metin and S. Özkar, *Int. J. Hydrogen Energy,* 2011, **36**, 1424− 1432.
37 H. Wang, Y. Zhao, F. Cheng, Z. Tao and J. Chen, *Catal. Sci. Technol.*, 2016, **6**, 3443−3448.